Population Switching and Charge Sensing in Quantum Dots: A Case for a Quantum Phase Transition

Moshe Goldstein,[1] Richard Berkovits,[1] and Yuval Gefen[2]

[1]*The Minerva Center, Department of Physics, Bar-Ilan University, Ramat-Gan 52900, Israel*

[2]*Department of Condensed Matter Physics, The Weizmann Institute of Science, Rehovot 76100, Israel*

(Received 26 August 2009; published 3 June 2010)

A broad and a narrow level of a quantum dot connected to two external leads may swap their respective occupancies as a function of an external gate voltage. By mapping this problem onto a multiflavored Coulomb gas we show that such population switching is not abrupt. However, trying to measure it by adding a third electrostatically coupled lead may render this switching an abrupt first order quantum phase transition. This is related to the interplay of the Mahan mechanism versus the Anderson orthogonality catastrophe, in similitude to the Fermi edge singularity. A concrete setup for experimental observation of this effect is also suggested.

DOI: 10.1103/PhysRevLett.104.226805 PACS numbers: 73.21.La, 72.10.Fk, 71.27.+a

The phenomenon of population switching (PS) [1–3] occurs in a discrete level quantum dot (QD)—e.g., a QD with one broad level and one narrow level. Upon a continuous variation of a plunger gate voltage the occupation numbers of the levels are inverted, cf. Fig. 1. This phenomenon is relevant to a wide range of experimentally observed effects, including the widely used technique of charge sensing [4] and, possibly, the occurrence of a large shot noise Fano factor through a QD [5], as well as correlated lapses [6] of the transmission phase through a QD [7,8]. One particularly intriguing question in this context is whether or not (at zero temperature) PS is abrupt, and hence constitutes a first order quantum phase transition (QPT).

In the following we address this question in the context of a two-level QD coupled to leads of spinless noninteracting electrons. This is mapped onto a system of two single-level QDs, each coupled to a single lead (cf. Fig. 2). We formulate the problem in terms of a multiflavored Coulomb gas (CG), perform a renormalization group (RG) analysis of this 15 parameter problem, and show that its low temperature behavior is akin to an antiferromagnetic Kondo problem; hence, no QPT occurs. This is dramatically changed when a third lead (e.g., a quantum point contact, QPC, serving as a charge sensor) is electrostatically coupled to one of the QDs. The model may then scale to the ferromagnetic Kondo problem, and by tuning the strength of the third lead coupling, one induces a QPT.

The problem at hand can be viewed within an even broader context. The features of the Fermi edge singularity are the result of the competition between the Anderson orthogonality catastrophe and the Mahan exciton physics [9]. The fact that the latter wins gives rise to the divergence at the x-ray absorption edge. Such an interplay is present here, too. Turning on the electrostatic coupling to the third lead increases the weight of the orthogonality catastrophe. The latter eventually wins, suppressing transitions between charge configurations before and after PS takes place. This implies a QPT between these two configurations. Our setup then serves as a handy laboratory which allows us to control and tune the relative strengths of two fundamental effects in many-body physics.

The original system of spinless electrons, made of a two (unequal) orbital level QD connected to two leads [cf. Fig. 2(a)], is described by the Hamiltonian $H = \tilde{H}_{\text{lead}} + \tilde{H}_{\text{dot}} + \tilde{H}_{\text{dot-lead}}$. We assume the leads to be noninteracting, and the dot-lead tunneling matrix elements $\tilde{V}_{i\ell}$ ($i = 1, 2$ and $\ell = L, R$ for left, right) to be real and possess left-right symmetry, $|\tilde{V}_{iL}| = |\tilde{V}_{iR}|$ (effects of asymmetry are discussed later). We will consider the more intricate case $\text{sgn}(\tilde{V}_{1L}\tilde{V}_{1R}\tilde{V}_{2L}\tilde{V}_{2R}) = -1$ [7]. We now map the original model onto a modified one consisting of two single-level QDs, cf. Fig. 2(b). The Fermi operators ψ_L and ψ_R of the new leads are made of symmetric and antisymmetric combinations of the original $\tilde{\psi}_L$ and $\tilde{\psi}_R$, respectively. The Hamiltonian is $H = \sum_\ell H_\ell + H_U$, with $H_\ell = H_{\ell,\text{lead}} + H_{\ell,\text{dot}} + H_{\ell,\text{dot-lead}}$, where $H_{\ell,\text{lead}}$ describes the Fermi liquid of the respective lead, $H_{\ell,\text{dot}} = \varepsilon_\ell d_\ell^\dagger d_\ell$ ($d_\ell^\dagger$ is the creation operator at dot ℓ), $H_{\ell,\text{dot-lead}} = V_\ell d_\ell^\dagger \psi_\ell(0) + \text{H.c.}$ with $V_L = \sqrt{2}|\tilde{V}_{1L}|$ and $V_R = \sqrt{2}|\tilde{V}_{2R}|$, and, finally, $H_U = U d_L^\dagger d_L d_R^\dagger d_R$. The dot-lead coupling gives rise to level widths $\Gamma_\ell = \pi|V_\ell|^2\rho_\ell$, where ρ_ℓ are the local densities of states.

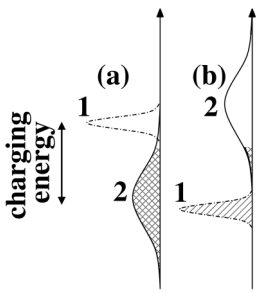

FIG. 1. Respective occupation of levels 1 and 2 (a) before and (b) after population switching has taken place.

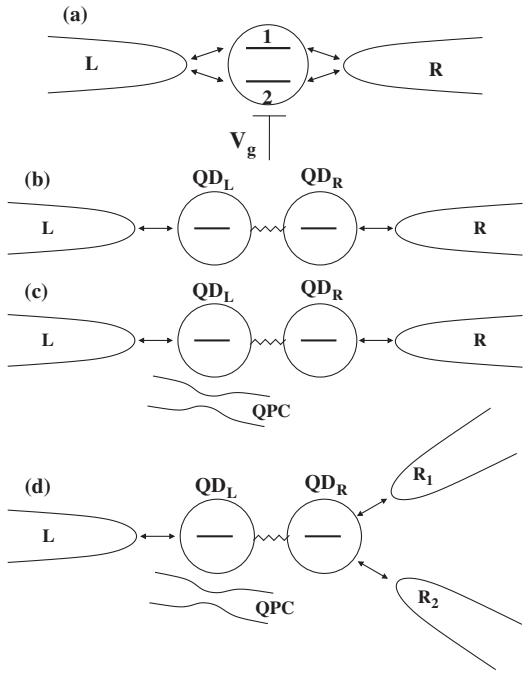

FIG. 2. The systems discussed: (a) the original model of a two-level quantum dot; (b) an equivalent model of two electrostatically coupled single-level QDs; (c) a third terminal (QPC) added; (d) right level tunnel-coupled to two leads.

Using standard techniques, we can rewrite the partition function as that of a classical multiflavor one-dimensional CG [10–13]. The imaginary time history of the system (a circle of circumference $1/T$, the inverse temperature) is divided into intervals in which the system is in one of four states spanning the filling configurations of the two dots: $\alpha = 00$, 10, 01, and 11 (cf. Fig. 3). The state α has dimensionless energy h_α. These intervals are separated by transition events, the CG particles. A transition from configuration α to β ($\alpha \neq \beta$) is associated with a fugacity $y_{\alpha\beta} = y_{\beta\alpha}$, and a two-component vector charge $\vec{e}_{\alpha\beta} = -\vec{e}_{\beta\alpha}$ (the two components correspond to the charge removed from the L and R leads, respectively, cf. Table I).

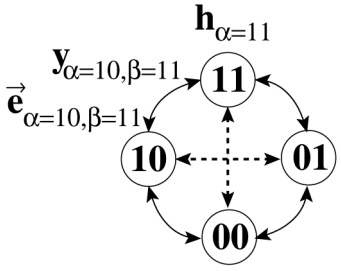

FIG. 3. Illustration of the parameters characterizing the CG [Eqs. (1) and (2)]: $h_{\alpha=11}/\xi$ is the energy associated with the state 11; its bare value is $(\varepsilon_L + \varepsilon_R + U)$. The transition depicted involves the fugacity $y_{\alpha=10,\beta=11}$ and the charge $\vec{e}_{\alpha=10,\beta=11}$, whose bare values are $\sqrt{\Gamma_R \xi/\pi}$ and (0, 1), respectively (see Table I). Dashed lines indicate couplings generated through RG iterations, e.g., $y_{10,01}$ (corresponding to $\rho J_{xy}/2$).

The partition function reads

$$Z = \sum_{N=0}^{\infty} \sum_{\alpha_i,\beta_i} y_{\alpha_1\beta_1} \cdots y_{\alpha_N\beta_N} \int_0^{1/T} \frac{d\tau_{2N}}{\xi} \cdots \int_0^{\tau_2-\xi} \frac{d\tau_1}{\xi} e^{-S(\{\tau_i,\alpha_i\})}, \tag{1}$$

where $\beta_i = \alpha_{i+1}$, $N+1 \equiv 1$, and ξ is a short-time cutoff. The classical CG action is

$$S(\{\tau_i, \alpha_i\}) = \sum_{i<j=1}^{N} \vec{e}_{\alpha_i\beta_i} \cdot \vec{e}_{\alpha_j\beta_j} V_C(\tau_j - \tau_i) + \sum_{i=1}^{N} h_{\beta_i} \frac{\tau_{i+1} - \tau_i}{\xi} \tag{2}$$

with $V_C(\tau - \tau') = \ln\{\pi T \xi / \sin[\pi T(\tau - \tau')]\}$. Bare values of the CG parameters are listed in Table I.

We can now write down a set of 15 RG equations for the Coulomb-gas parameters (valid to second order in the fugacities but otherwise exact; here $\kappa_{\alpha\beta} \equiv |\vec{e}_{\alpha\beta}|^2$ and $\kappa^{\alpha}_{\beta\gamma} \equiv \kappa_{\alpha\beta} + \kappa_{\alpha\gamma} - \kappa_{\beta\gamma}$) [10,11]:

$$\frac{dy_{\alpha\beta}}{d\ln\xi} = \frac{2 - \kappa_{\alpha\beta}}{2} y_{\alpha\beta} + \sum_{\gamma} y_{\alpha\gamma} y_{\gamma\beta} e^{(h_\alpha + h_\beta)/2 - h_\gamma}, \tag{3}$$

$$\frac{d\kappa_{\alpha\beta}}{d\ln\xi} = -\sum_{\gamma} y^2_{\alpha\gamma} e^{h_\alpha - h_\gamma} \kappa^{\alpha}_{\beta\gamma} - \sum_{\gamma} y^2_{\beta\gamma} e^{h_\beta - h_\gamma} \kappa^{\beta}_{\alpha\gamma}, \tag{4}$$

$$\frac{dh_\alpha}{d\ln\xi} = h_\alpha - \sum_{\gamma} y^2_{\alpha\gamma} e^{h_\alpha - h_\gamma} + \frac{1}{4} \sum_{\beta,\gamma} y^2_{\beta\gamma} e^{h_\beta - h_\gamma}. \tag{5}$$

We now address the parameter regime in the vicinity of population switching. This requires $|\varepsilon_L - \varepsilon_R| < |\Gamma_L - \Gamma_R|$. Defining $\varepsilon_0 = (\varepsilon_L + \varepsilon_R)/2$, we have, in the Coulomb-blockade valley, $|\varepsilon_0|$, $\varepsilon_0 + U \gg \Gamma_L$, Γ_R. The RG flow is then divided into three stages: (i) $\xi^{-1} \gg \max(|\varepsilon_0|, \varepsilon_0 + U)$, all four filling configurations take equal part in the RG flow; (ii) $\min(|\varepsilon_0|, \varepsilon_0 + U) \ll \xi^{-1} \ll \max(|\varepsilon_0|, \varepsilon_0 + U)$, the higher energy configuration between 00 and 11 drops out; (iii) $\xi^{-1} \ll \min(|\varepsilon_0|, \varepsilon_0 + U)$, only configurations 10 and 01 survive. In this last stage we are left with a CG of only a single type of transition—equivalent to the single channel anisotropic Kondo model [10]. The main effect of the first two stages of the flow is to establish the $10 \rightleftharpoons 01$ transition (via virtual processes through the dou-

TABLE I. Parameters appearing in the CG expansion [Eqs. (1) and (2)], corresponding to the system depicted in Fig. 2(b).

Fugacities	Charges	Energies
$y_{00,10} = \sqrt{\Gamma_L \xi/\pi}$	$\vec{e}_{00,10} = (1, 0)$	$h_{00} = 0$
$y_{00,01} = \sqrt{\Gamma_R \xi/\pi}$	$\vec{e}_{00,01} = (0, 1)$	$h_{10} = \varepsilon_L \xi$
$y_{10,11} = \sqrt{\Gamma_R \xi/\pi}$	$\vec{e}_{10,11} = (0, 1)$	$h_{01} = \varepsilon_R \xi$
$y_{01,11} = \sqrt{\Gamma_L \xi/\pi}$	$\vec{e}_{01,11} = (1, 0)$	$h_{10} = (\varepsilon_L + \varepsilon_R + U)\xi$
$y_{10,01} = 0$	$\vec{e}_{10,01} = (-1, 1)$	
$y_{00,11} = 0$	$\vec{e}_{00,11} = (1, 1)$	

bly occupied and unoccupied states, 11 and 00), and to renormalize the corresponding parameters.

The resulting Kondo model has the following couplings, to leading order in Γ_ℓ (parameters refer to bare values) [13]:

$$\rho J_z = 1 - \frac{\kappa_{10,01}}{2} + \left[\frac{\Gamma_L}{2\pi}\left(\frac{Q_{2\kappa_{00,10}}(|\varepsilon_L|\xi)}{|\varepsilon_L|}\kappa^{10}_{01,00} + \frac{Q_{2\kappa_{01,11}}([\varepsilon_L+U]\xi)}{\varepsilon_L+U}\kappa^{01}_{10,11}\right) + \{L\leftrightarrow R, 10\leftrightarrow 01\}\right], \tag{6}$$

$$\rho J_{xy} = \frac{2\sqrt{\Gamma_L\Gamma_R}}{\pi}\left[\frac{Q_{\kappa_{00,10}+\kappa_{00,01}}(|\varepsilon_0|\xi)}{|\varepsilon_0|} + \frac{Q_{\kappa_{10,11}+\kappa_{01,11}}([\varepsilon_0+U]\xi)}{\varepsilon_0+U}\right], \tag{7}$$

$$H_z = \varepsilon_L - \varepsilon_R - \frac{\Gamma_L}{\pi}[P_{2\kappa_{00,10}}(|\varepsilon_L|\xi) - P_{2\kappa_{01,11}}([\varepsilon_L+U]\xi)] + \frac{\Gamma_R}{\pi}[P_{2\kappa_{00,01}}(|\varepsilon_R|\xi) - P_{2\kappa_{10,11}}([\varepsilon_R+U]\xi)], \tag{8}$$

where $P_a(x) = \Gamma(1-a/2)/x^{1-a/2}$, $Q_a(x) = (1-a/2)P_a(x)$. For the system discussed thus far (cf. Table I) we find

$$\rho J_z = \frac{\Gamma_L}{\pi}\left(\frac{1}{\varepsilon_L+U} + \frac{1}{|\varepsilon_L|}\right) + \frac{\Gamma_R}{\pi}\left(\frac{1}{\varepsilon_R+U} + \frac{1}{|\varepsilon_R|}\right), \tag{9}$$

$$\rho J_{xy} = \frac{2\sqrt{\Gamma_L\Gamma_R}}{\pi}\left(\frac{1}{\varepsilon_0+U} + \frac{1}{|\varepsilon_0|}\right), \tag{10}$$

$$H_z = \varepsilon_L - \varepsilon_R - \frac{\Gamma_L}{\pi}\ln\frac{\varepsilon_L+U}{|\varepsilon_L|} + \frac{\Gamma_R}{\pi}\ln\frac{\varepsilon_R+U}{|\varepsilon_R|}, \tag{11}$$

in agreement with the poor man's scaling of Refs. [8]. H_z will change sign as the gate voltage is swept across the Coulomb-blockade valley, provided that $|\varepsilon_L - \varepsilon_R| < |\Gamma_L - \Gamma_R|$; hence the spin projection $\langle S_z\rangle$ will also change sign, implying a PS. Since J_{xy} and J_z are antiferromagnetic, they flow to strong coupling, so the PS will be continuous over the scale of the Kondo temperature, $T_K = \frac{\sqrt{U(\Gamma_L+\Gamma_R)}}{\pi}\exp[\frac{\pi\varepsilon_0(U+\varepsilon_0)}{2U(\Gamma_L-\Gamma_R)}\ln(\frac{\Gamma_L}{\Gamma_R})]$.

The problem becomes much more intriguing when an electrostatically coupled third lead (e.g., a QPC charge sensor) is introduced, cf. Fig. 2(c). The sensor adds to the Hamiltonian a term $H_S = H^S_{\rm lead} + U_S{:}\psi^\dagger_S(0)\psi_S(0){:}(d^\dagger_L d_L - \frac{1}{2})$, the Hamiltonian of a free lead plus an interaction term. One may reemploy the Coulomb-gas formalism, but now $\vec{e}_{\alpha\beta}$ consists of three components [11,13]. Denoting the population of dot L in state α by $n_{L\alpha}$, the third component of $\vec{e}_{\alpha\beta}$ is given by $(n_{L\beta} - n_{L\alpha})\delta_S/\pi$, with $\delta_S = 2\tan^{-1}(\pi\rho_S U_S/2)$ being the change in phase shift of the electronic wave functions of the QPC caused by a change in the population of dot L, and ρ_S the corresponding local density of states. The resulting RG equations [Eqs. (3)–(5)] and their general solution [Eqs. (6)–(8)] are as before. Now, however, the bare values are $\kappa_{00,01} = \kappa_{10,11} = 1$, $\kappa_{00,10} = \kappa_{01,11} = 1 + (\delta_S/\pi)^2$, and $\kappa_{00,10} = \kappa_{01,11} = 2 + (\delta_S/\pi)^2$. At low energies we are still left with an effective Kondo model. The main effect of the QPC would be to reduce ρJ_z by $(\delta_S/\pi)^2/2$, through the first term on the right-hand side of Eq. (6). It may then drive the system to the weak coupling (ferromagnetic Kondo) regime, and render the PS an abrupt first order QPT. For this to happen the QPC charge sensitivity needs to not be too high; we require $\rho_S U_S \sim \{\sum_\ell \Gamma_\ell[(\varepsilon_\ell + U)^{-1} + |\varepsilon_\ell|^{-1}]\}^{1/2} \ll 1$. The transition at $J_z = -J_{xy}$ between the continuous and discontinuous PS regimes is of the Kosterlitz-Thouless type.

Our analysis here can be put in a more general context. Around the point where PS takes place we need to consider only pseudospin up (10) and down (01) states. Let us first ignore the QPC. Processes in which an electron (or a hole) hops in and out of a level give rise to an effective repulsive interaction between the charge of each level and the charge at the end of the nearby lead, of the form $\sum_\ell U_\ell{:}\psi^\dagger_\ell(0)\psi_\ell(0){:}(d^\dagger_\ell d_\ell - \frac{1}{2})$, $U_\ell = |V_\ell|^2[(\varepsilon_\ell + U)^{-1} + |\varepsilon_\ell|^{-1}]$. These correspond [by Eq. (9)] to the usual Kondo $J_z S_z s_z(0)$ coupling. A process of the type $10 \rightleftharpoons 01$ (pseudospin flip, J_{xy} process) contributes to the hybridization of these two configurations, hence (if relevant) to a smearing of the PS. The aforementioned effective repulsion introduces two competing elements into this dynamics. On the one hand, $10 \rightleftharpoons 01$ involves a change in the lead's state and, hence, is suppressed by the Anderson orthogonality catastrophe. On the other hand, an electron settling in one of the levels has prepared itself a hole in the lead into which it can hop (a Mahan exciton). This facilitates tunneling out and in (by reducing the Pauli blockade), thus enhancing hybridization of $10 \rightleftharpoons 01$. The overall scaling dimension is given by $d_{xy} = 1 - (\delta_L + \delta_R)/\pi + (\delta^2_L + \delta^2_R)/2\pi^2$, where $\delta_\ell = 2\tan^{-1}(\pi\rho_\ell U_\ell/2)$ is the phase-shift change in lead ℓ as a result of the $10 \rightleftharpoons 01$ transition. In this expression for d_{xy} the linear (quadratic) term in δ_ℓ denotes the contribution of the Mahan (Anderson) physics [14]. Since $\delta_\ell < \pi$, $d_{xy} < 1$ (relevant), so PS is a continuous crossover. However, when a third lead is added, the scaling dimension is increased by $(\delta_S/\pi)^2/2$, the extra orthogonality associated with the QPC. This may make the Anderson effect dominant, and the population switching abrupt.

As mentioned above, the QPC can be thought of as a measuring device (detector of the population of one QD). At the same time, it is the introduction of this QPC which drives the population switching from a mere crossover to a genuine QPT. How, then, could one differentiate between having and not having a QPT? A solution can be achieved by attaching an additional lead to, say, the right QD [cf. Fig. 2(d)]. Our analysis remains unchanged, provided V_R is replaced by $\sqrt{|V_{R1}|^2 + |V_{R2}|^2}$, where $V_{R1(2)}$ is the

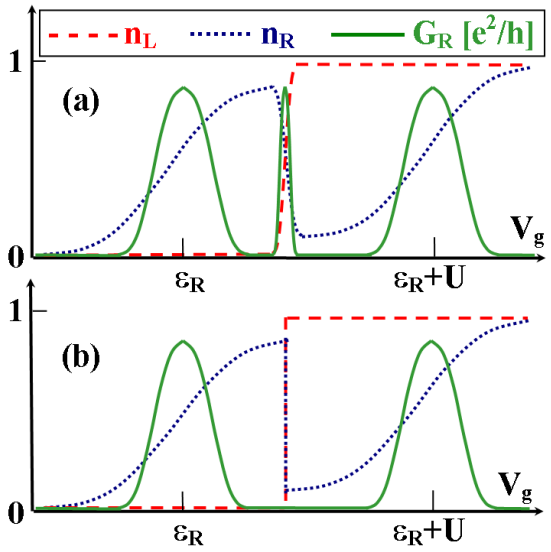

FIG. 4 (color online). Schematic behavior of the level populations (n_L and n_R) and the conductance through the right level (taking it as the wider one) for (a) continuous or (b) abrupt switching. See the text for further details.

tunneling amplitude to lead $R_{1(2)}$. Now, however, one could measure the conductance G_R through the right level, which will be related to the average population of the latter, n_R, by the Friedel sum rule: $G_R = \frac{e^2}{h}(\frac{2|V_{R1}V_{R2}|}{|V_{R1}|^2+|V_{R2}|^2})^2 \sin^2(\pi n_R)$. Thus, in the regime of continuous switching, in addition to the two usual Coulomb-blockade peaks (of width Γ_R) one will find a "correlation induced resonance" (CIR) [7,8] of width $UT_K/|\Gamma_R - \Gamma_L|$ [Fig. 4(a)]; as the electrostatic coupling to the QPC increases, T_K will decrease in a Kosterlitz-Thouless fashion, $\ln T_K \sim (U_S^* - U_S)^{-1/2}$, until we reach the abrupt population switching regime at $U_S \geq U_S^*$. From that point on, the CIR disappears [Fig. 4(b)].

The analysis presented here, while specifically tackling the ubiquitous physics of population switching and charge sensing, is close to earlier studies of QPTs involving two-level systems [15], including Kondo models coupled to Ohmic baths [12,16]. Here we have found that PS is inherently not abrupt, but in attempting to measure it with a third terminal (a QPC) one may induce a QPT. The system at hand is an appealing laboratory to modify and control at will such effects as Mahan exciton, Anderson orthogonality catastrophe, and Fermi edge singularity [9].

There are several obvious extensions to our analysis. The absence of left-right symmetry in the original model [Fig. 2(a)] implies a finite interdot hopping t_{LR} in the equivalent model, Fig. 2(b) [8]. This simply expresses the possible transition of an electron from one level to the other through the leads, and will smear the PS, as first noted in the last of Refs. [1]. Finite temperature will also have a rounding effect. Thus, in the proposed experiment one could try to follow the manner of decrease of the width of the CIR as a function of U_S, before it disappears as soon as $T_K < T$. Finally, the spinful analogue of the model can be shown to display a similar behavior in the first Coulomb-blockade valley. All these issues will be elaborated elsewhere [13].

We thank D. I. Golosov and J. von Delft for useful discussions. Financial support from the Adams Foundation of the Israel Academy of Science, EU project GEOMDISS, GIF, ISF (Grants No. 569/07 and No. 715/08), the Minerva Foundation, and Schwerpunkt Spintronics SPP 1285 is gratefully acknowledged.

[1] G. Hackenbroich, W. D. Heiss, and H. A. Weidenmüller, Phys. Rev. Lett. **79**, 127 (1997); R. Baltin *et al.*, Eur. Phys. J. B **10**, 119 (1999); P. G. Silvestrov and Y. Imry, Phys. Rev. Lett. **85**, 2565 (2000); Phys. Rev. B **65**, 035309 (2001).
[2] R. Berkovits, F. von Oppen, and Y. Gefen, Phys. Rev. Lett. **94**, 076802 (2005).
[3] J. König and Y. Gefen, Phys. Rev. B **71**, 201308(R) (2005); M. Sindel, A. Silva, Y. Oreg, and J. von Delft, *ibid.* **72**, 125316 (2005).
[4] M. Field *et al.*, Phys. Rev. Lett. **70**, 1311 (1993).
[5] O. Zarchin *et al.*, Phys. Rev. Lett. **98**, 066801 (2007).
[6] R. Schuster *et al.*, Nature (London) **385**, 417 (1997); M. Avinun-Khalish *et al.*, *ibid.* **436**, 529 (2005).
[7] A. Silva, Y. Oreg, and Y. Gefen, Phys. Rev. B **66**, 195316 (2002); V. Meden and F. Marquardt, Phys. Rev. Lett. **96**, 146801 (2006); D. I. Golosov and Y. Gefen, Phys. Rev. B **74**, 205316 (2006); C. Karrasch *et al.*, Phys. Rev. Lett. **98**, 186802 (2007); M. Goldstein and R. Berkovits, New J. Phys. **9**, 118 (2007); M. Goldstein *et al.*, Phys. Rev. B **79**, 125307 (2009).
[8] J. Martinek *et al.*, Phys. Rev. Lett. **91**, 127203 (2003); H.-W. Lee and S. Kim, *ibid.* **98**, 186805 (2007); V. Kashcheyevs *et al.*, Phys. Rev. B **75**, 115313 (2007); Phys. Rev. Lett. **102**, 136805 (2009); P. G. Silvestrov and Y. Imry, Phys. Rev. B **75**, 115335 (2007).
[9] G. D. Mahan, *Many-Particle Physics* (Kluwer, New York, 2000).
[10] G. Yuval and P. W. Anderson, Phys. Rev. B **1**, 1522 (1970); F. D. M. Haldane, J. Phys. C **11**, 5015 (1978).
[11] J. L. Cardy, J. Phys. A **14**, 1407 (1981); Q. Si and G. Kotliar, Phys. Rev. B **48**, 13881 (1993).
[12] A. Kamenev and Y. Gefen, Phys. Rev. B **54**, 5428 (1996); arXiv:cond-mat/9708109.
[13] M. Goldstein, R. Berkovits, and Y. Gefen (to be published).
[14] H. E. Türeci *et al.*, arXiv:0907.3854; A. Weichselbaum, M. Goldstein, Y. Gefen, and J. von Delft (to be published).
[15] A. J. Leggett *et al.*, Rev. Mod. Phys. **59**, 1 (1987).
[16] N. Andrei, G. T. Zimányi, and G. Schön, Phys. Rev. B **60**, R5125 (1999); M. Garst *et al.*, *ibid.* **69**, 214413 (2004); K. Le Hur, Phys. Rev. Lett. **92**, 196804 (2004); M.-R. Li and K. Le Hur, *ibid.* **93**, 176802 (2004); L. Borda, G. Zaránd, and P. Simon, Phys. Rev. B **72**, 155311 (2005); M. T. Glossop and K. Ingersent, Phys. Rev. Lett. **95**, 067202 (2005); S. Florens *et al.*, Phys. Rev. B **75**, 155321 (2007); C.-H. Chung *et al.*, *ibid.* **76**, 235103 (2007); S. Kirchner and Q. Si, Phys. Rev. Lett. **100**, 026403 (2008).